RESEARCH PAPER

A three-dimensional microfluidic tumor cell migration assay to screen the effect of anti-migratory drugs and interstitial flow

Johann Kalchman · Shingo Fujioka · Seok Chung ·
Yamato Kikkawa · Toshihiro Mitaka · Roger D. Kamm ·
Kazuo Tanishita · Ryo Sudo

Abstract Most anti-cancer drug screening assays are currently performed in two dimensions, on flat, rigid surfaces. However, there are increasing indications that three-dimensional (3D) platforms provide a more realistic setting to investigate accurate morphology, growth, and sensitivity of tumor cells to chemical factors. Moreover, interstitial flow plays a pivotal role in tumor growth. Here, we present a microfluidic 3D platform to investigate behaviors of tumor cells in flow conditions with anti-migratory compounds. Our results show that interstitial flow and its direction have significant impact on migration and growth of hepatocellular carcinoma cell lines such as HepG2 and HLE. In particular, HepG2/HLE cells tend to migrate against interstitial flow, and their growth increases in interstitial flow conditions regardless of the flow direction. Furthermore, this migratory activity of HepG2 cells is enhanced when they are co-cultured with human umbilical vein endothelial cells. We also found that migration activity of HepG2 cells attenuates under hypoxic conditions. In addition, the effect of Artemisinin, an anti-migratory compound, on HepG2 cells was quantitatively analyzed. The microfluidic 3D platform described here is useful to investigate more accurately the effect of anti-migratory drugs on tumor cells and the critical influence of interstitial flow than 2D culture models.

2D	Two dimensional
HCC	Hepatocellular carcinoma
ART	Artemisinin
PDMS	Poly-dimethylsiloxane
VEGF	Vascular endothelial growth factor
bFGF	Basic fibroblast growth factor
HUVEC	Human umbilical vein endothelial cell
PBS	Phosphate-buffered saline

J. Kalchman · K. Tanishita · R. Sudo
School of Integrated Design Engineering,
Keio University, Yokohama, Japan

J. Kalchman
Ecole Centrale de Lille, Villeneuve-d'Ascq, France

S. Fujioka · K. Tanishita · R. Sudo (✉)
Department of System Design Engineering, Keio University,
3-14-1 Hiyoshi, Kohoku-ku, Yokohama 223-8522, Japan
e-mail: sudo@sd.keio.ac.jp

S. Chung
School of Mechanical Engineering,
Korea University, Seoul, Korea

Y. Kikkawa
Laboratory of Clinical Biochemistry, Tokyo University
of Pharmacy and Life Sciences, Tokyo, Japan

T. Mitaka
Department of Tissue Development and Regeneration,
Research Institute for Frontier Medicine, Sapporo Medical
University School of Medicine, Sapporo, Japan

R. D. Kamm
Departments of Mechanical Engineering and Biological
Engineering, Massachusetts Institute of Technology,
Cambridge, USA

1 Introduction

Tumor cell migration is a critical factor in the context of metastatic activity, and when a tumor has metastasized, patients have less than 50 % chance to survive for more than a year (Decaestecker et al. 2007). In the formation of

🖄 Springer

metastases, tumor cells first migrate from the primary tumor site to vessels as single cells or masses before entering the circulation which transports them to distant parts of the body. Primary liver cancers are usually treated with pro-apoptotic anti-cancer drugs (Kinoshita et al. 2000; Haga et al. 2003; Sekharam et al. 2003). However, by the time metastases occur, tumor cells have already acquired a resistance to these drugs. Therefore, an anti-migratory strategy targeting metastatic tumor cells is highly desired (Decaestecker et al. 2007).

Most anti-cancer drug screening assays have been performed in two-dimensional (2D) culture models with cells plated onto a flat surface, either treated plastic or, in some cases, an extracellular matrix (ECM) analog. Nevertheless, there is increasing evidence suggesting that three-dimensional (3D) culture models in which the cells are immersed in ECM are essential to investigate accurate cellular morphology, growth, and reaction of tumor cells to chemical factors (Gurski et al. 2010). One common alternative is the use of in vivo models to investigate drug effects, but these often suffer from the inability to make direct observations and to regulate the local microenvironment; therefore, the ability to understand all phenomena in vivo is greatly compromised. In contrast, in vitro models have been increasingly developed to allow for greater control of the microenvironment and closer monitoring of the critical phenomena. Therefore, 3D microfluidic systems have emerged as powerful and controllable tools for manipulating biochemical and biophysical microenvironments of tumors. The most common 3D cell culture models are composed of a collagen gel scaffold where cell aggregates can grow naturally in a mechanical microenvironment that mimics that of a tumor in vivo (Gurski et al. 2010). In order to analyze behaviors of cells in the invasion and metastasis, in vitro models must properly mimic the tumor microenvironments, and many parameters affecting tumor cell behaviors need to be screened. In particular, interstitial flow, biochemical compounds, ECM chemistry and mechanics and local oxygen levels around cells are all key factors.

The influence of these parameters was previously documented using various 2D and 3D models (Decaestecker et al. 2007). Particularly, interstitial flow, the convective transport of fluid through tissue ECM, has been demonstrated to affect the morphology and migration of various cell types including endothelial cells and tumor cells (Haessler et al. 2011). It is also known that interstitial flow is related to the metastasis of tumors and the guidance of tumor cell movement (Shieh and Swartz 2011). Therefore, recent studies have reproduced interstitial flow in microfluidic systems to investigate its influence on tumor behaviors (Haessler et al. 2011; Polacheck et al. 2011).

Previous in vitro models have been studying each of tumor microenvironment parameters separately. However, combining these parameters is important for controlling tumor cell behaviors. Our microfluidic tumor cell migration assay screened the effect of anti-migratory drugs in a 3D platform, where interstitial flow, biochemical parameters and ECM could be controlled precisely and simultaneously. In particular, we used interstitial flow to enhance the migration of tumor cells against the flow and observe more accurate tumor cell reaction to anti-migratory drugs. Moreover, our system could be used in a hypoxic condition and in the co-culture of tumor and other cells in combination with anti-migratory drugs.

Here, we present a microfluidic 3D platform to investigate behaviors of hepatocellular carcinoma (HCC), such as HepG2 and HLE cells, in flow conditions with soluble biochemical factors. This microfluidic device has been used for hepatocyte-endothelial cell co-culture in our previous study (Sudo et al. 2009). The microfluidic system has many advantages over the conventional methods used for tumor invasion studies such as culture inserts: abilities to monitor 3D cell migration, to create co-culture with defined cellular locations, and to culture tumor cells in controlled biochemical and biophysical microenvironments. The purpose of this study is to investigate HCC cell behaviors under interstitial flow conditions in combination with additional key factors such as anti-migratory drug, endothelial cells and hypoxia. Our results demonstrate that interstitial flow and its direction exerts a significant influence on migration and growth of HCC cells. HCC cells tend to migrate against interstitial flow, and their growth is increased in the presence of interstitial flow regardless of flow direction. Furthermore, the effect of artemisinin (ART), an anti-migratory compound, on HepG2 cells was quantitatively analyzed, and the influence of hypoxia was also investigated. We propose a new approach using a 3D microfluidic device to study the effect of anti-migratory drugs on tumor cells in a controlled tumor microenvironment such as interstitial flow conditions.

2 Materials and methods

2.1 Preparation of microfluidic devices

The shape and dimension of the gel region were designed to produce capillary forces sufficient to confine and support the injected gel solution. The width of the gel scaffold, 600 μm, was selected to withstand the pressures and shear stresses associated with interstitial flow across the gel and to promote interactions between cells cultured in the two separate microchannels (Fig. 1a). Channel width and height were
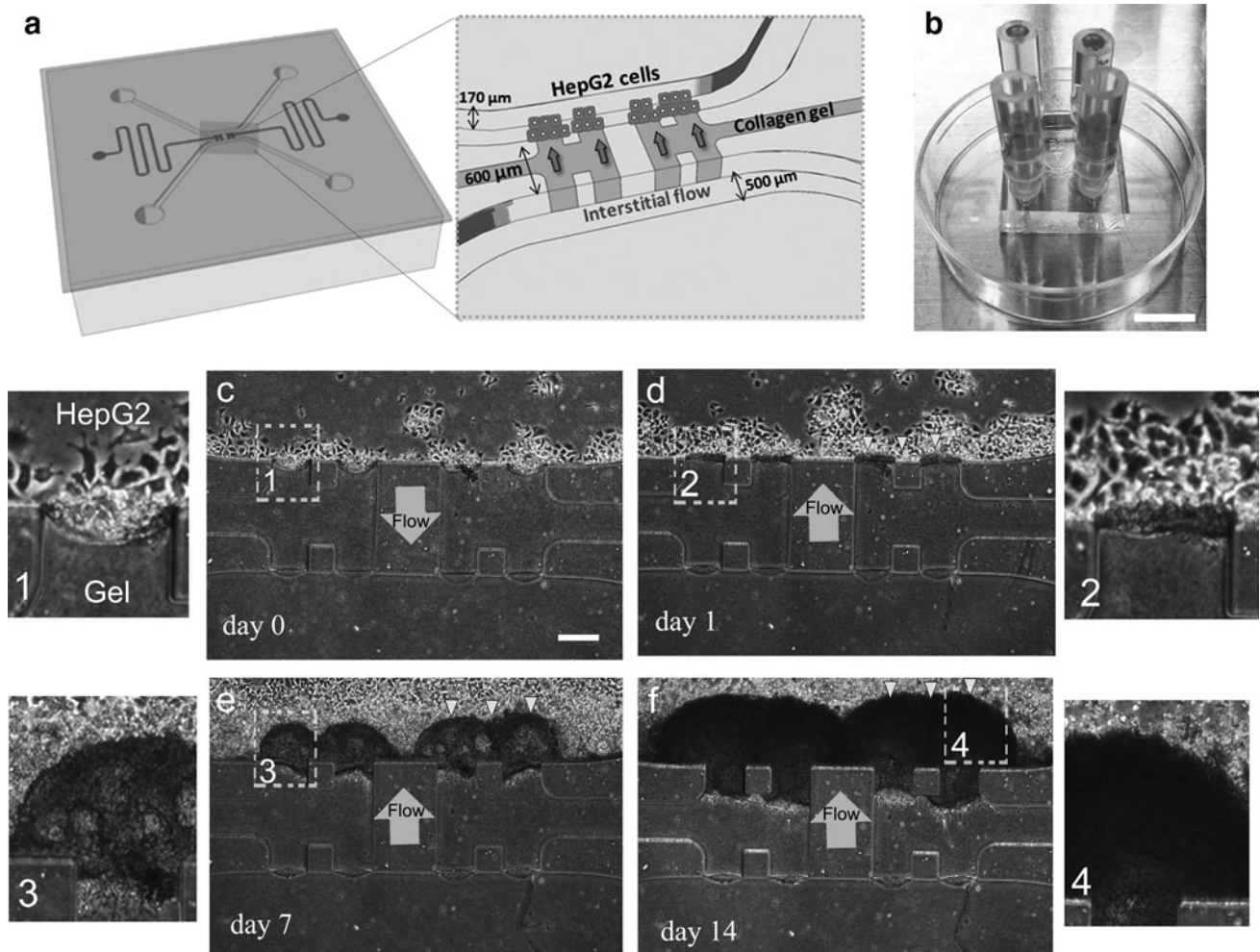
Fig. 1 The microfluidic platform for investigating HepG2/HLE migration. **a** Schematic diagram and dimension of the microfluidic device made of PDMS. Two parallel microchannels are formed between a micropatterned PDMS device and a coverglass. Collagen gel is located between the microchannels with a mechanical support of PDMS posts. **b** A picture of the microfluidic device cultured in a flow condition. Reservoirs were connected to microchannels, and interstitial flow across the collagen gel was generated by pressure difference between two microchannels. **c–f** Phase-contrast images taken on *day 0*, *day 1*, *day 7* and *day 14* of culture. Enlarged images corresponding to the regions indicated by the *rectangles* in **c–f** were shown in *1–4*. HepG2 cells were seeded in the device on day 0, and forward flow was applied to facilitate the 3D structure formation (an *arrow*, **c**). Single HepG2 cells were stacked on the sidewall of the gel or attached on the channel surface (*1*). On day 1, the flow is inversed to remove debris (an *arrow*, **d**). Cells formed clusters but external cells still showed single cell outlines (*2*). On day 2, cells were cultured in three types of experimental condition, forward flow, reverse flow, or static. Here, reverse flow is applied until day 14 (*arrows*, **e**, **f**). HepG2 cells formed tumor masses with relatively smooth surface on days 7 and 14 (*3*, *4*). *Scale bars* 1 cm (**b**) and 200 μm (**c**)

selected to reduce shear stress on the cells during medium replacement and to provide sufficient area for cell adhesion to the sidewall of the gel scaffold (Sudo et al. 2009). Details of the device fabrication process were described recently (Shin et al. 2012). Briefly, the microfluidic device was made of poly-dimethylsiloxane (PDMS; Silgard 184, Dow Chemical, Midland, MI, USA) and was produced via soft lithography with SU-8 patterned wafers. The PDMS device with the surface patterning of microchannels was bonded to a coverglass to form microchannels. After the microchannels were coated with poly-D-lysine (Sigma-Aldrich, St. Louis, MO, USA), prepolymerized type I collagen gel solution

(2 mg/ml, pH 7.4; BD Biosciences, San Jose, CA, USA) was injected into the gel region through the injection ports and placed in the humidified 5 % CO_2 incubator at 37 °C for 30 min to polymerize the solution. Microchannels were filled with culture medium, and the microfluidic devices were kept in the incubator until use.

2.2 Culture of HepG2, HLE and human umbilical vein endothelial cells

Two human HCC cell lines, HepG2 and HLE, were purchased from Health Science Research Resource Bank

(Osaka, Japan). HepG2 and HLE cells were derived from well- and poorly differentiated HCC, respectively. The cells were cultured in HCC media: DMEM (Invitrogen, Carlsbad, CA, USA) supplemented with 10 % FBS, 20 ng/ml vascular endothelial growth factor (VEGF), 20 ng/ml basic fibroblast growth factor (bFGF) and antibiotics. Human umbilical vein endothelial cells (HUVECs) were purchased from Lonza (Walkerville, MD, USA) and cultured in HU-VEC media: EGM-2 (Lonza) supplemented with 10 % FBS, 20 ng/ml VEGF and 20 ng/ml bFGF. HUVECs were expanded in culture dishes within seven passages and seeded into microfluidic devices. For co-culture experiments, HU-VECs were added to HepG2/HLE culture on day 3. A 1:1 mixture of the HCC medium and HUVEC medium was used for both co-culture and monoculture, and the medium was replaced every day.

2.3 Protrusion formation assay and interstitial flow generation

HepG2 or HLE cell suspensions (3×10^6 cells/ml, 20 μl per device) were prepared and seeded into one of the two microchannels (Fig. 1a). Details of the cell seeding process were described recently (Shin et al. 2012). Briefly, the device was tipped on its side and kept in the incubator for 30 min to allow cells to attach to the sidewall of the collagen gel scaffold. Returning the device to horizontal, cells were then cultured under constant flow condition in order to promote cell adhesion to the gel. Interstitial flow was generated as described in our previous study (Sudo et al. 2009). Briefly, medium reservoirs were inserted into the channel outlets (Fig. 1b), and an interstitial flow across the collagen gel was generated by a pressure difference of 5 mm H_2O.

Forward flow, flow from HepG2 cells' side to the other side, was applied immediately after cell seeding. On the next day (day 1), the interstitial flow was inversed (reverse flow) in the manner described above, but with the pressure difference reversed. These first 2 days were necessary to generate a 3D structure of the tumor mass. From day 3, the cells were cultured either in forward flow, reverse flow, or under static conditions. Culture medium was replaced every day. Phase-contrast images were taken every day to observe HepG2/HLE protrusions and HepG2/HLE mass expansion. The number of newly formed protrusions longer than 100 μm and detaching from the tumor mass was counted every day using phase-contrast images. The sum of the protrusion numbers during culture periods was calculated and graphically shown for all experimental conditions. For HepG2-HUVEC co-culture experiments, HUVEC cell suspension (1×10^6 cells/ml, 20 μl per device) was prepared and seeded into the other microchannel on day 2.

2.4 Anti-migratory compounds-ART

An anti-migratory compound, ART (Sigma-Aldrich) was added to the culture media on both sides. HepG2 cells were seeded in the microfluidic devices and cultured in the medium supplemented with 200 μM ART. Culture medium was replaced every day, and anti-migratory effects of ART were monitored by phase-contrast microscopy. The cells were also seeded in a culture dish and cultured in the medium supplemented with ART to investigate the effect of ART on cell–cell adhesion.

2.5 Immunofluorescence staining of cultured cells

Cells were fixed in 4 % paraformaldehyde for 30 min and treated with 0.1 % Triton X-100 for 40 min. After rinsing with phosphate-buffered saline (PBS), the cells were incubated with Block Ace (Dainippon Pharma, Tokyo, Japan) for 90 min. HCC cells were then incubated for 2 h with mouse anti-pan cadherin antibody. After rinsing with PBS, the cells were incubated for 2 h with Alexa Fluor 488 or 594-conjugated anti-mouse antibodies. Then after rinsing with PBS, the cells were incubated for 2 h with Alexa Fluor 488 or 594-conjugated phalloidin. Nuclei were counterstained with 4′,6-diamidino-2-phenylindole (Sigma-Aldrich) or propidium iodide (Invitrogen). The z-axis series of fluorescence images was obtained using a confocal laser-scanning microscope (LSM700; Carl Zeiss, Hallbergmoos, Germany).

2.6 Hypoxia experiments

To investigate the effect of hypoxia on the behavior of HepG2 cells, microfluidic devices were placed in an incubator with the oxygen tension adjusted to 5 %. As a control experiment, some microfluidic devices were cultured in 21 % (air) oxygen. Culture medium was replaced every day for both hypoxic and normoxic conditions.

2.7 Statistical analyses

Data are presented as mean $\pm$ SD. A Student's t test was used to test for differences, which were considered statistically significant at error levels of ***$p < 0.001$.

3 Results

3.1 HepG2/HLE cell protrusions and migration

To investigate HepG2/HLE cell behaviors in a controlled microenvironment, HepG2 cells were cultured in the 3D microfluidic platform (Fig. 1a, b). The cells attached on the
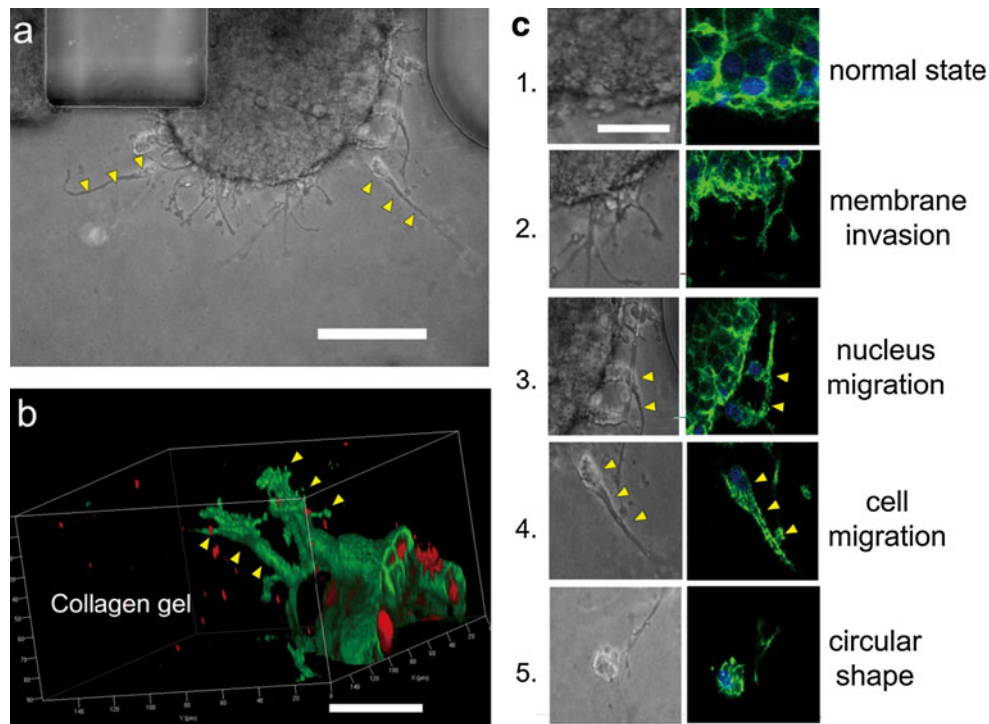
Fig. 2 Five steps of liver cancer cell migration observed in the microfluidic platform. **a** A phase-contrast image of a HepG2 cell cluster with extending cytoplasmic protrusions (*arrowheads*). The image was taken on day 9 cultured in the reverse flow condition. HepG2 cells formed a 3D tumor mass before penetrating and migrating into collagen gel. **b** A 3D projection image of confocal fluorescent images showing HepG2 migration and tumor mass. The cells were fixed on day 9 and stained for actin (*green*) and nuclei (*red*). Note that the cells extended 3D protrusions into collagen gel

(*arrowheads*). **c** Corresponding fluorescent and phase-contrast images of the representative five steps of HepG2 migration into collagen gel. Cells were stained for actin (*green*) and nuclei (*blue*). *Step 1*: cells are part of a tumor mass in a normal state. *Step 2*: a cell membrane starts spreading into collagen gel. *Step 3*: a nucleus moves toward the spreading membrane. *Step 4*: a cell detaches from the tumor mass and migrates into collagen gel. *Step 5*: cell shape is back to its circular shape. *Arrowheads* indicate protrusions of HepG2 cells. *Scale bars* 100 μm (**a**), 50 μm (**b**), and 50 μm (**c**)

sidewall of the collagen gel and cultured in forward flow to form HepG2 cell aggregates (arrow, Fig. 1c). An enlarged image showed that single HepG2 cells were stacked on the sidewall of the collagen gel (enlarged image 1, Fig. 1c). On day 1, the cells formed small aggregates on the sidewall of the collagen gel (arrowheads, Fig. 1d). HepG2 clusters with visible single cell outlines could also be observed (enlarged image 2, Fig. 1d). The cells were then cultured in reverse flow to remove debris within the aggregates (arrow, Fig. 1d). In all experimental conditions, the cells were cultured in the forward flow followed by reverse flow in the first 2 days. From day 2, the cells were cultured either under forward flow, reverse flow or static conditions. Here, we showed the representative image of the cells cultured in the reverse flow condition (Fig. 1e, f). We observed the growth of HepG2 cell aggregates to form 3D tumor masses during 14 days of culture (Fig. 1f). Enlarged images showed the HepG2 cluster with relatively smooth surface (enlarged images 3, 4, Fig. 1e, f).

We found that HepG2 cells extended protrusions from the 3D tumor masses (arrowheads, Fig. 2a). Three-dimensional projection images revealed that this HepG2 cell

migration occurred in 3D (arrowheads, Fig. 2b). Furthermore, in the development of HepG2 cell aggregates in the microfluidic platform, tumor cell movements were divided into several steps (Fig. 2c). First, HepG2 cells aggregated and formed a 3D tumor mass, in which each cell showed cuboidal/circular shape (Fig. 2c1). After day 5 or 6, the next step of movements occurred where the cell membrane spread into collagen gel (Fig. 2c2). Thereafter, nuclei moved toward the membrane protrusion (Fig. 2c3). The cells finally detached from the tumor mass to start migration into the collagen gel (Fig. 2c4). A few days later, the cells changed their morphology to their original circular shape but still continued to migrate (Fig. 2c5).

3.2 The effect of interstitial flow on HepG2/HLE cell protrusions

To further investigate the HepG2 cell migration, cells were cultured in three different conditions: forward flow, reverse flow, and static conditions. When HepG2 cells were cultured in the forward flow condition, few HepG2 cell protrusions were observed during 14 days of culture (Fig. 3a). In the

Fig. 3 Effect of interstitial flow on HepG2/HLE protrusions. Representative phase-contrast images of HepG2 cells cultured in forward flow (**a**), static (**b**), or reverse flow (**c**) conditions. Images were taken on day 14 and showed that reverse flow increased the extent of HepG2 protrusions into collagen gel. *Scale bars* 200 μm (**a**) and 100 μm (*1*). **d** Quantitative analysis of the number of HepG2 protrusions on day 14 cultured in forward flow, static and reverse flow conditions (***$p < 0.001$). **e** Quantitative analysis of the number of HLE protrusions on day 14 in forward flow, static and reverse flow conditions (***$p < 0.001$)
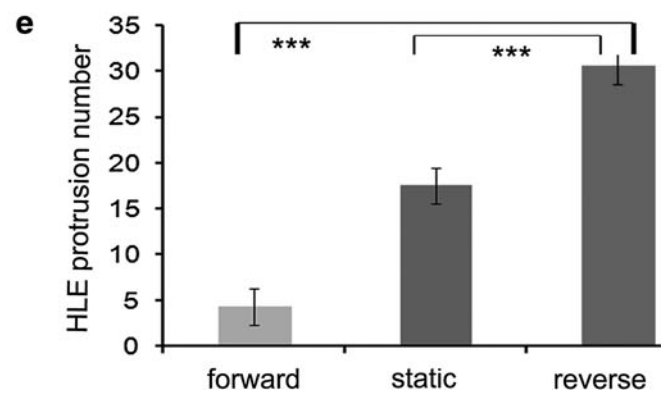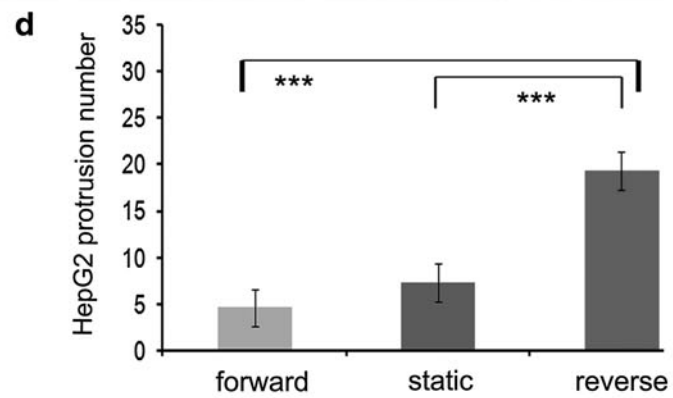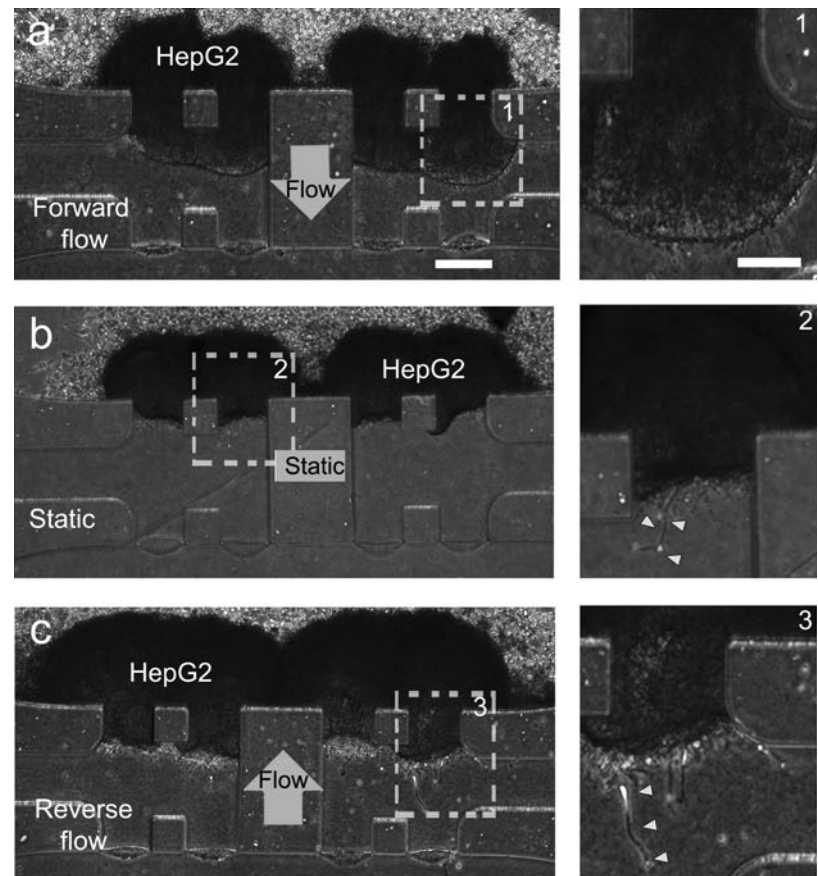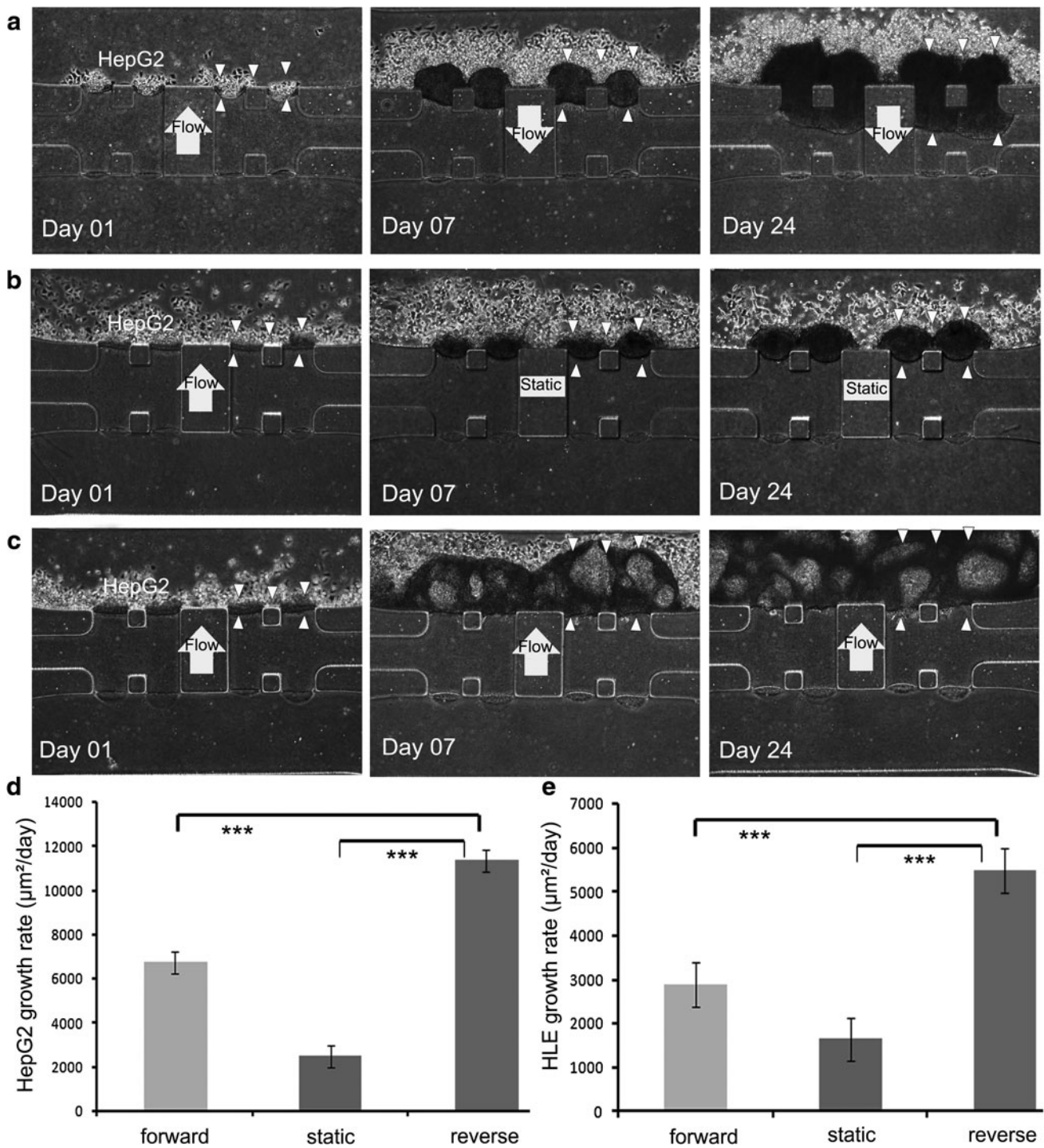
Fig. 4 Effect of interstitial flow on HepG2/HLE growth rate. Corresponding phase-contrast images of HepG2 cells on days 1, 7 and 24, cultured in forward flow (**a**), static (**b**), and reverse flow (**c**) conditions. *Arrowheads* indicate the edge of growing HepG2 clusters. **d** Quantitative analysis of HepG2 tumor mass growth rate (μm^2/day) cultured in forward flow (**a**), static (**b**) and reverse flow (**c**) conditions. The area of the tumor mass in 2D projection image was measured. The *graph* presents the average growth rate within 24 days of culture (***$p < 0.001$). **e** Quantitative analysis was also carried out for HLE (***$p < 0.001$)

static condition, some HepG2 cell protrusions were observed (arrowheads, Fig. 3b). In contrast to these conditions, when the cells were cultured in the reverse flow condition, HepG2 cells actively migrated into a collagen gel (arrowheads, Fig. 3c). The quantitative analysis revealed that the number of HepG2 cell protrusions in the reverse flow condition increased 2.9-fold compared to the static condition, and fourfold compared to the forward flow condition (Fig. 3d).
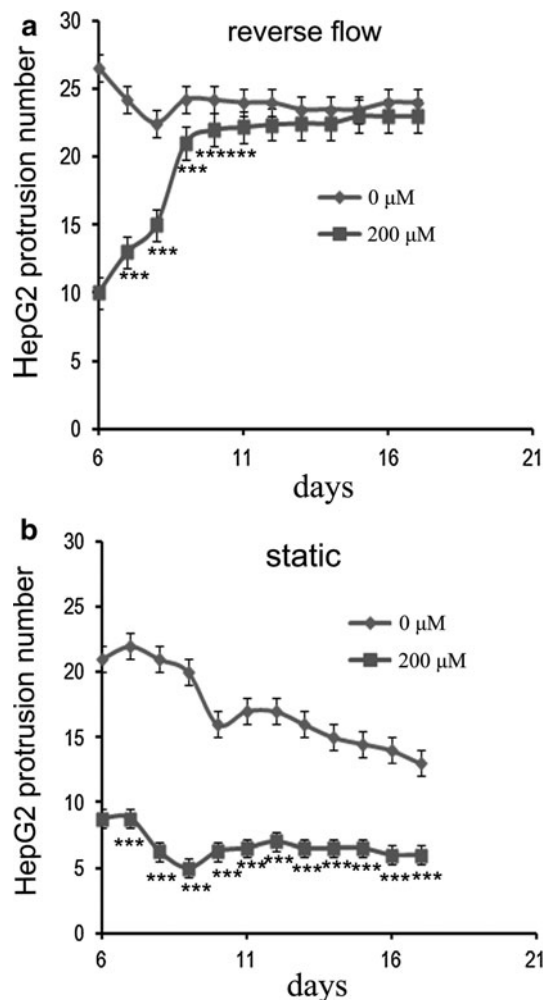
Fig. 5 Quantitative analysis of the effect of ART on HepG2 cell protrusions. **a** The number of HepG2 cell protrusions in the reverse flow condition with/without ART. The *graph* presents the number of protrusions over the culture period until day 17. The graph shows the anti-migratory effect of ART on HepG2 cells and a decrease in efficiency with time in culture (***$p < 0.001$). **b** The number of HepG2 cell protrusions in the static condition with/without ART. The graph shows the anti-migratory effect of ART on HepG2 was retained at least until day 17 (***$p < 0.001$)

Since HepG2 cells were well-differentiated HCC cells, we also used HLE cells, poorly differentiated HCC cells, to confirm this phenomenon. Quantitative analysis revealed that HLE cells showed the same phenomenon of protrusion to the interstitial flow applications (Fig. 3e). The number of HLE cell protrusions in the reverse flow condition increased 1.8-fold compared to the static condition and 7.5-fold compared to the forward flow condition.

3.3 The effect of interstitial flow on the growth of HepG2/HLE masses

The same type of experiments using various interstitial flow conditions allowed clear observation of the tumor mass

growth. When HepG2 cells were cultured in the forward flow condition, the cells formed a tumor mass, which was continuously expanding during 24 days of culture (Fig. 4a). The tumor mass expanded not only into the microchannel, but also toward the collagen gel (arrowheads, Fig. 4a). On the other hand, when HepG2 cells were cultured in the static condition, the tumor mass gradually expanded (Fig. 4b) but did not expand into collagen gel (arrowheads, Fig. 4b). When HepG2 cells were cultured in the reverse flow condition, the tumor mass rapidly expanded, and the whole width of the microchannel was occupied by the tumor mass by day 24 (arrowheads, Fig. 4c). However, the tumor mass did not expand into collagen gel even by day 24. Quantitative analysis revealed that interstitial flow dramatically promoted tumor growth (Fig. 4d). In both forward and reverse flow conditions, the tumor mass attained a larger size than in the static condition by day 24. More precisely, HepG2 tumor mass growth rate in the reverse flow condition increased by 4.8 times compared to the static condition, while that in the forward flow condition increased by 2.3 times compared to the static condition (Fig. 4d). This phenomenon was also confirmed with HLE cells. HLE tumor mass growth rate in the reverse flow condition increased by 3 times compared to the static condition, while that in the forward flow condition increased by 1.7 times compared to the static condition (Fig. 4e).

3.4 Application of an anti-migratory compound, ART to the HepG2 3D culture model

To demonstrate one application of our microfluidic HCC 3D culture model, an anti-migratory compound, ART was added to the culture medium and HepG2 cell behaviors were analyzed. HepG2 cells were seeded and cultured with ART under reverse flow or static conditions, where the HepG2 cell protrusions were observed. Quantitative analysis revealed that the number of HepG2 protrusions in the reverse flow condition decreased until day 10 (Fig. 5a). In particular, ART treatment decreased the number of HepG2 protrusions by 40 % on day 7. However, this anti-migratory effect gradually decreased during culture. The anti-migratory effect of ART was progressively attenuated to the point that there was no significant difference between ART-treated cells and control cells after day 10. On the other hand, the number of HepG2 protrusions in the static condition also decreased by 40 % on day 7, but this decrease sustained at least until day 17 (Fig. 5b).

3.5 ART improved HepG2 cell–cell adhesion by renewing cadherin

HepG2 cells were also cultured in a 2D condition with 100 μM ART, and immunofluorescent staining was carried

Fig. 6 Effect of ART on cadherin expression in HepG2 cells. Immunofluorescent images for cadherin in HepG2 cells with (**a**) or without (**b**) ART administration. Cells were fixed on day 4, stained for cadherin, and observed with a ×40 objective lens. *Images* show a higher cadherin expression in HepG2 cells with ART administration compared to control experiment where the cells were culture without ART (control). *Scale bar* 20 μm (**a**). **c** Quantitative analysis of the cadherin expression intensity in HepG2 cells with/without ART administration (***$p < 0.001$)
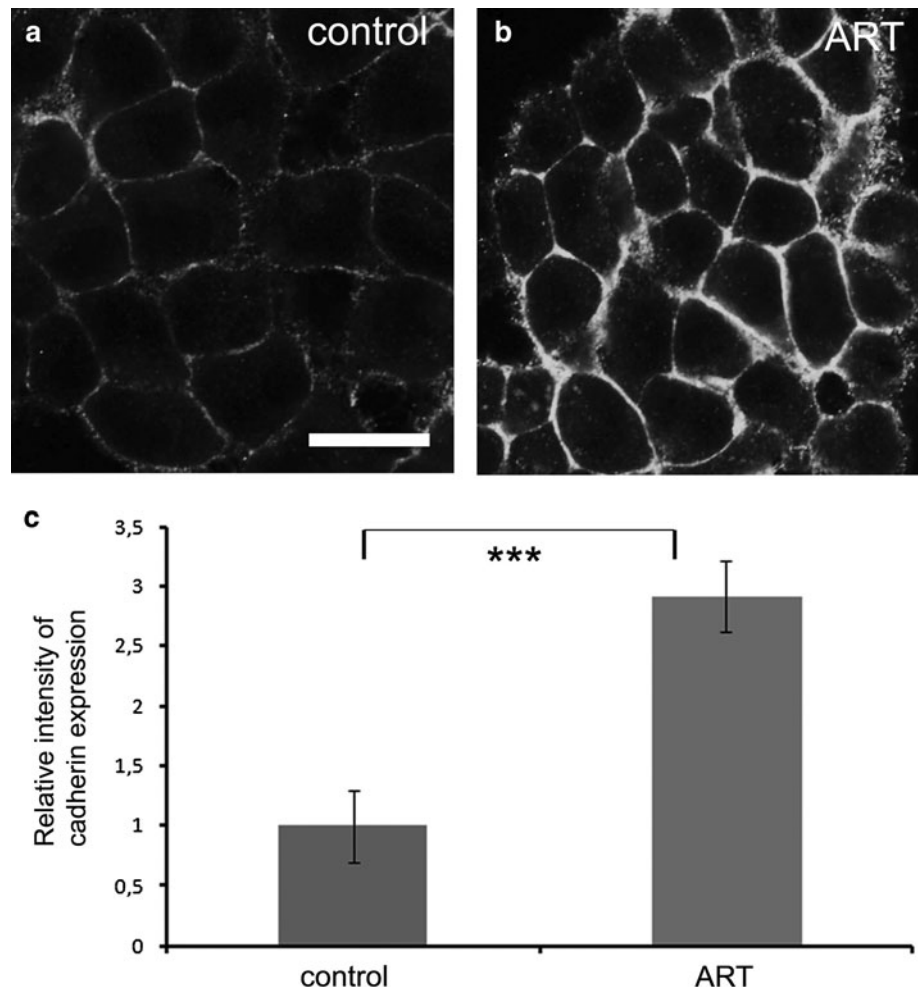
out to investigate the effect of ART on HepG2 cell–cell adhesion. The results revealed that HepG2 cells showed low fluorescent intensity of cadherin at cell–cell borders in a control experiment (Fig. 6a). However, when the cells were cultured with ART, intense cadherin staining was detected between HepG2 cells (Fig. 6b). Quantitative analysis of the fluorescent intensity also confirmed this phenomenon. Fluorescent intensity of cadherin with ART treatment was more than threefold higher than control (Fig. 6c).

3.6 Potential applications to HCC-HUVEC co-culture and hypoxic condition

Finally, the HepG2/HLE cell culture model was extended to co-culture with HUVEC or hypoxic conditions to further demonstrate potential applications of the model. This culture model can readily be extended to co-culture since our microfluidic device has two microchannels (Fig. 7a). In this experiment, HUVECs were added to HepG2 culture on day

2 to start HepG2-HUVEC co-culture, and the cells were cultured until day 14 (Fig. 7b–d). The cells were cultured in the reverse flow or static conditions. In both conditions, co-culture results showed a higher number of HepG2 cell protrusions compared to monoculture (Fig. 7e). Protrusion numbers increased in HepG2-HUVEC co-culture by 1.6 times both in the static and reverse flow conditions compared to monoculture. This phenomenon was also confirmed in the experiment with HLE cells. The number of HLE cell protrusions in HLE-HUVEC co-culture increased by 2.6 times in the static condition, and by 2.7 times in the reverse flow condition compared to monoculture (Fig. 7f).

To investigate the effect of a hypoxic environment on HCC cell protrusions, we implemented two experiments with HepG2 cells under normal oxygen condition (21 % O2) and under hypoxic condition (5 % O2). The results revealed that HepG2 cell protrusions in reverse flow condition attenuated by the hypoxic condition (Fig. 7g). The number of HepG2 cell protrusions in hypoxic condition decreased by 70 % compared to normal oxygen condition.

Fig. 7 Potential extensions of the microfluidic culture system to co-culture and hypoxic conditions. **a** Schematic diagram of the HUVEC-HepG2 co-culture created in a microfluidic platform. **b–d** Corresponding phase-contrast images of the co-culture system in reverse flow conditions on days 1, 2, and 8. The enlarged image corresponding to the rectangle *1* in **d**) was shown in *1*. *Arrowheads* indicate HepG2 cell protrusions. **e** Quantitative results of the number of HepG2 protrusions in static or reverse flow conditions in HepG2 monoculture and HepG2-HUVEC co-culture. Significant difference appears in the reverse flow condition, demonstrating that HUVEC presence enhanced HepG2 protrusions (***$p < 0.001$). **f** The number of HLE protrusions was also quantified for HLE monoculture and HLE-HUVEC co-culture (***$p < 0.001$). **g** The number of HepG2 protrusions in normoxic (21 % O_2) and hypoxic (5 % O_2) conditions. HepG2 protrusions were attenuated in hypoxic conditions (***$p < 0.001$)
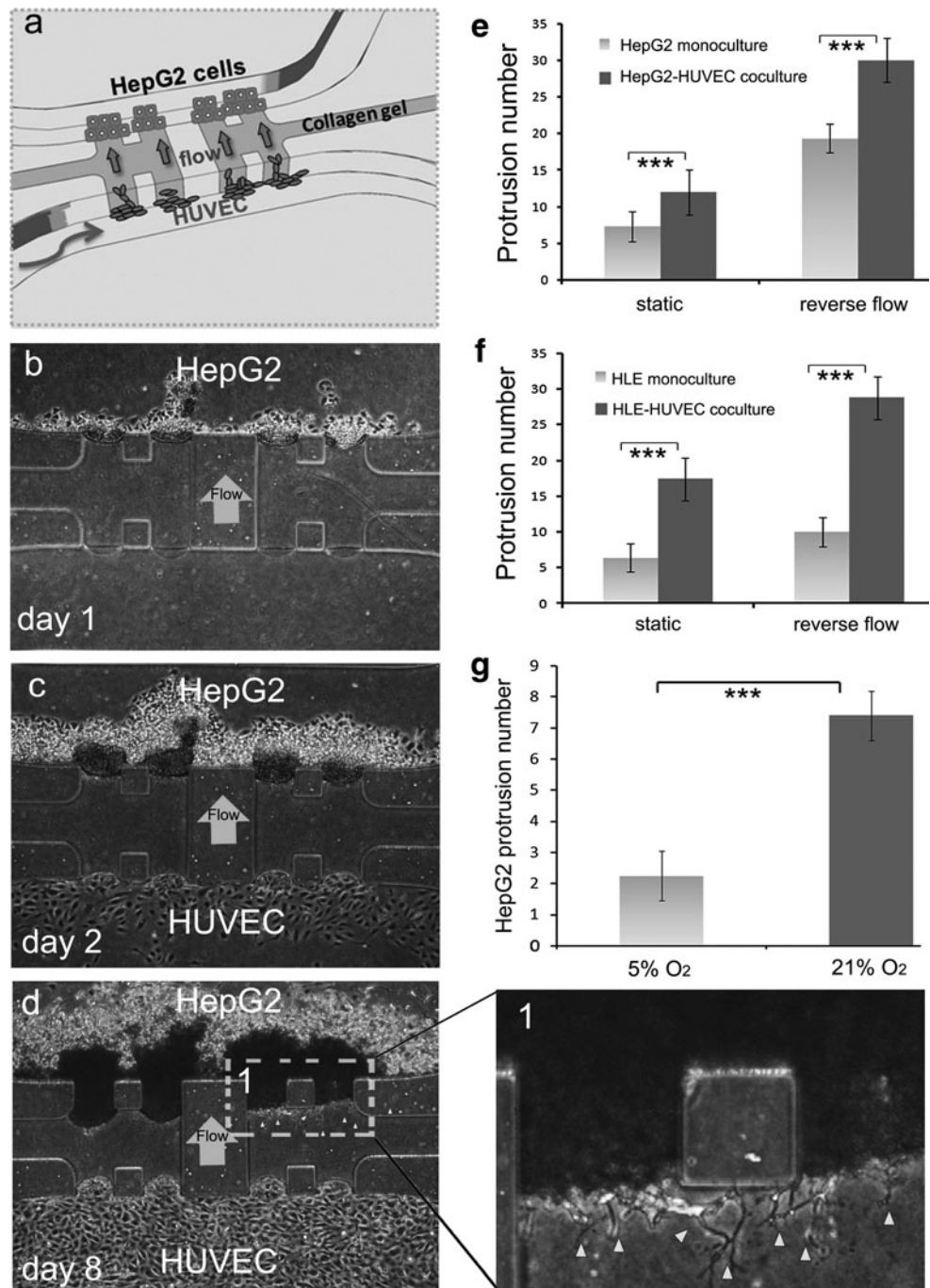
4 Discussion

4.1 3D HCC cell migrations in a controlled microenvironment

A 3D microfluidic platform was developed in this study for investigating 3D migration of HCC cells, such as HepG2 and HLE cells, in flow conditions with the treatment of anti-migratory drugs. HepG2/HLE cells first gathered to form small aggregates and then expanded to form 3D tumor masses. Thereafter, the cells migrated in 3D from the tumor mass. The formation of the 3D tumor mass with protrusions into collagen gel may mimic in vivo tumor microenvironments compared to conventional 2D culture models.

Our microfluidic platform, transparent and biocompatible to maintain high cell viability, allowed us to clearly monitor cellular morphogenesis by phase-contrast microscopy. We identified several steps in the process of the HCC cell migration. During these steps, tumor cells attached to

ECM via cell surface receptors, locally degraded the ECM, protruded the cell membranes following the movement of their nuclei and then detached from the tumor mass (Liotta 1986). Metastasis may take place by repeating these events.

4.2 Effect of interstitial flow on HCC cells

In the present study, interstitial flow application significantly affected both migration and growth of HepG2/HLE cells. In particular, both forward and reverse flow conditions enhanced the growth of HepG2/HLE cells. Interstitial flow has been previously observed to affect cellular behavior and morphogenesis. In addition, interstitial fluid pressure in most tumors is high, as supported by the significantly positive correlation between interstitial fluid pressure and the enlargement of tumor size (Gutmann et al. 1992; Raju et al. 2008).

An important finding was that HepG2/HLE cells tended to migrate against the interstitial flow. Two mechanisms have been proposed to explain why interstitial flow increases tumor cell motility. One, which is consistent with our observations, is an integrin-mediated mechanism and dependent on interstitial flow direction and strength (Polacheck et al. 2011). It has also been observed, at relatively lower cell densities, that tumor cells migrate in the direction of the flow. Haessler et al. (2011) reported that an increase in interstitial flow was found in the microenvironment within a tumor mass and that the flow influenced tumor cell migration. In particular, autologous chemotaxis, a directed cell migration induced by interstitial flow, has been identified as a potentially important mechanism; in this case, cancer cells migrate in the direction of the flow (Shieh and Swartz 2011; Fleury et al. 2006; Shields et al. 2007). In both cases, it is important to note that interstitial flow dramatically increased the motility of tumor cells. In the case of autologous chemotaxis, activation of the CCR7 receptor by the CCL21 ligand self-secreted by tumor cells causes cell polarization and stimulates migration in the direction of the flow. The direction of tumor cell migration can thus be determined by the balance of these competing mechanisms, suggesting that cell density, interstitial flow rate, and CCR7 receptor availability are key factors for controlling migratory activity of tumor cells (Polacheck et al. 2011).

In the present experiments, we used both well- and poorly differentiated HCC cells, HepG2 and HLE, respectively. These cells responded to the interstitial flow in a similar fashion, where the number of HepG2/HLE cell protrusions increased in the reverse flow condition. However, the number of cell protrusions was much higher in HLE cells than that in HepG2 cells. These results indicate that the degree of differentiation of the cells may be important to regulate the motility of tumor cells. In normal liver, neighboring hepatocytes are bound with E-cadherin. It is thought that poorly differentiated HLE cells express less E-cadherin compared to well-differentiated HepG2 cells, which would contribute to the enhanced migratory capacity of HLE cells. In addition, it was previously demonstrated that pathophysiological behaviors of tumor cells and their growth pattern were different depending on the degree of cellular differentiation (Zheng et al. 2003; Xin et al. 2001). The shape of the tumor cell protrusion, which depends on the integrin-mediated cell adhesion to ECM (Garcia et al. 1999), was also related to the degree of cellular differentiation.

4.3 Application for anti-migratory drug screening

ART is a natural product isolated from the plant *Artemisia annua L.*, or sweet wormwood and has anti-migratory effects on various tumor cell lines, including HCC cells (Hou et al. 2008). We tested this compound in our 3D HepG2 culture model to provide support for the use of this model for drug screening. Since the device can be readily visualized by phase-contrast microscopy, HepG2 cell migrations were monitored and analyzed with or without ART administration. As expected, ART treatment significantly reduced the number of HepG2 cell protrusions. We also confirmed that ART-treated HepG2 cells recovered their cadherin localization at cell–cell borders. This recovery of the cell–cell adhesion helps to explain the decrease of the HepG2 cell migration because of the role of E-cadherin in determining tumor progression (Jeanes et al. 2008). Tumor cells tend to progress through an epithelial–mesenchymal transition marked by a loss of E-cadherin expression, which results in an increase of metastatic potential (Yang et al. 2005).

Our results demonstrate that the inhibitory effect of ART on cell motility due to interstitial flow gradually wanes in culture, while it is maintained under static conditions. This suggests that interstitial flow may be critical for the efficacy of ART on HepG2 cells. The previous study suggested a correlation between response to the drug treatment and interstitial pressures (Curti et al. 1993). An important finding in the experiment using ART was that HepG2 cells in a 3D microfluidic platform exhibited a different response to ART compared to 2D studies. In 2D culture, the inhibitory effect of ART on HepG2 cells became stronger with time in culture (Weifeng et al. 2011). The attenuation of ART effect observed in this study may be due to the accelerated growth of HepG2 cells in interstitial flow conditions, resulting in a higher consumption of ART, a newly developed resistance to the drug, or a physical response. In addition, both 3D structure and the properties of the ECM exert important effects on drug efficacy, influencing tissue architecture and cancer cell

behavior and function compared to 2D models (Weigelt et al. 2009). Therefore, 3D models such as our microfluidic platform may be crucial to properly assess anti-cancer drugs and their effect on tumor progression and metastasis.

4.4 Extensions of the model to more pathophysiological conditions

Tumor cell behaviors are controlled by multiple factors in the tumor microenvironment in vivo. It is therefore important to consider interactions between tumor cells and other components of the tumor microenvironment such as the existence of endothelial cells. Co-culture of HepG2/ HLE cells and HUVECs led to the observation that HU-VECs increase the number of HepG2/HLE cell protrusions compared to monoculture. It has long been recognized that tumor cells induce angiogenesis in vivo (Hanahan and Weinberg 2011); however, it is not well understood if endothelial cells induce migration of tumor cells. Our results suggested that HUVECs secrete biochemical factors that enhance HepG2/HLE cell migration. Further investigations are needed to clarify the mechanisms of the HUVEC influence on tumor cells.

Our model was also used to analyze tumor cell migration in a hypoxic condition. The level of oxygenation is another key factor to be considered while investigating tumor cell migration since hypoxia is well known to alter tumor cell behavior (Chan and Giaccia 2007). Our results demonstrated that the number of HepG2 cell protrusions is reduced in hypoxia. A similar phenomenon was observed in another experiment using different tumor cells, in which hypoxia significantly decreased invasion of prostate cancer cells (Ackerstaff et al. 2007).

In conclusion, our microfluidic device offers the potential to analyze various factors that control tumor cell behavior, for example, interstitial flow, anti-migratory compounds, co-culture, and hypoxic conditions. This device is useful to investigate more accurately the effect of anti-migratory drugs on HCC cells and the critical influence of interstitial flow than 2D culture models. Pharmaceutical studies could therefore benefit from using a more physiological culture model to screen and assess novel anti-cancer drugs. In addition, in the future, one could use this strategy for personalized medicine in which numerous anti-cancer treatments could be assessed on the patients' own tumor cells to choose the most efficient drug for their particular tumor.

References

Ackerstaff E, Artemov D, Gillies RJ, Bhujwalla ZM (2007) Hypoxia and the presence of human vascular endothelial cells affect prostate cancer cell invasion and metabolism. Neoplasia 9:1138–1151

Chan DA, Giaccia AJ (2007) Hypoxia, gene expression, and metastasis. Cancer Metastasis Rev 26:333–339

Curti BD, Urba WJ, Alvord G, Janik JE, Smith JW 2nd, Madara K, Longo DL (1993) Interstitial pressure of subcutaneous nodules in melanoma and lymphoma patients: changes during treatment. Cancer Res 53:2204–2207

Decaestecker C, Debeir O, Van Ham P, Kiss K (2007) Can anti-migratory drugs be screened in vitro? A review of 2D and 3D assays for the quantitative analysis of cell migration. Med Res Rev 27:149–176

Fleury ME, Boardman KC, Swartz MA (2006) Autologous morphogen gradients by subtle interstitial flow and matrix interactions. Biophys J 91:113–121

Garcia AH, Vega MD, Boettiger D (1999) Modulation of cell proliferation and differentiation through substrate-dependent changes in fibronectin conformation. Mol Biol Cell 10:785–798

Gurski LA, Petrelli NJ, Jia X, Farach-Carson MC (2010) 3D Matrices for anti-cancer drug testing and development. Oncol Issues 25:20–25

Gutmann R, Leunig M, Feyh J, Goetz AE, Messmer K, Kastenbauer E, Jain RK (1992) Interstitial hypertension in head and neck tumors in patients: correlation with tumor size. Cancer Res 52:1993–1995

Haessler U, Teo JCM, Foretay D, Renaud P, Swartz MA (2011) Migration dynamics of breast cancer cells in a tunable 3D interstitial flow chamber. Integr Biol. doi:10.1039/C1IB00128K

Haga A, Funasaka T, Niinaka Y, Raz A, Nagase H (2003) Autocrine motility factor signaling induces tumor apoptotic resistance by regulations Apaf-1 and Caspase-9 apoptosome expression. Int J Cancer 107:707–714

Hanahan D, Weinberg RA (2011) Hallmarks of cancer: the next generation. Cell 144:646–674

Hou J, Wang D, Zhang R, Wang H (2008) Experimental therapy of hepatoma with artemisinin and its derivatives: in vitro and in vivo activity, chemosensitization, and mechanisms of action. Clin Cancer Res 14:5519–5530

Jeanes A, Gottardi CJ, Yap AS (2008) Cadherins and cancer: how does cadherin dysfunction promote tumor progression? Oncogene 27:6920–6929

Kinoshita K, Taupin DR, Itoh H, Podolsky DK (2000) Distinct pathways of cell migration and antiapoptotic response to epithelial injury: structure-function analysis of human intestinal trefoil factor. Mol Cell Biol 20:4680–4690

Liotta LA (1986) Tumor invasion and metastase: role of the extracellular matrix. Cancer Res 46:1–7

Polacheck WJ, Charest JL, Kamm RD (2011) Interstitial flow influences direction of tumor cell migration through competing mechanisms. Proc Natl Acad Sci USA 108:11115–11120

Raju B, Haug SR, Ibrahim SO, Heyeraas KJ (2008) High interstitial fluid pressure in rat tongue cancer is related to increased lymph vessel area, tumor size, invasiveness and decreased body weight. J Oral Pathol Med 37:137–144

Sekharam M, Zhao H, Sun M, Fang Q, Zhang Q, Yuan Z, Dan HC, Boulware D, Cheng JQ, Coppola D (2003) Insulin-like growth

factor-1 receptor enhances invasion and induces resistance to apoptosis of colon cancer cells through the Akt/Bcl-XL pathway. Cancer Res 63:7708–7716

Shieh AC, Swartz MA (2011) Regulation of tumor invasion by interstitial fluid flow. Phys Biol 8:015012

Shields JD, Fleury ME, Yong C, Tomei AA, Randolph GJ, Swartz MA (2007) Autologous chemotaxis as a mechanism of tumor cell homing to lymphatics via interstitial flow and autocrine CCR7 signaling. Cancer Cell 11:526–538

Shin Y, Han S, Jeon JS, Yamamoto K, Zervantonakis IK, Sudo R, Kamm RD, Chung S (2012) Microfluidic assay to analyze cellular morphogenesis that can incorporate hydrogels. Nat Protoc 7:1247–1259

Sudo R, Chung S, Zervantonakis IK, Vickerman V, Toshimitsu Y, Griffith LG, Kamm RD (2009) Transport-mediated angiogenesis in 3D epithelial coculture. FASEB J 23:2155–2164

Weifeng T, Feng S, Xiangji L, Changqing S, Zhiquan Q, Huazhong Z, Peining Y, Yong Y, Mengchao W, Xiaoqing J, Wan-Yee L (2011) Artemisinin inhibits in vitro and in vivo invasion and metastasis of human hepatocellular carcinoma cells. Phytomedicine 18:158–162

Weigelt B, Lo AT, Park CC, Gray JW, Bissell MJ (2009) HER2 signaling pathway activation and response of breast cancer cells to HER2-targeting agents is dependent strongly on the 3D microenvironment. Breast Cancer Res Treat 122:35–43

Xin Y, Li XL, Wang YP, Zhang SM, Zheng HC, Wu DY, Zhang YC (2001) Relationship between phenotypes of cell-function differentiation and pathobiological behavior of gastric carcinomas. World J Gastroenterol 7:53–59

Yang Z, Rayala S, Nguyen D, Vladlamudi RK, Chen S, Kumar R (2005) Pak1 phosphorylation of snail, a master regulator of epithelial-to-mesenchyme transition, modulates snail's subcellular localization and functions. Cancer Res 65:3179–3184

Zheng HC, Li YL, Sun JM, Yang XF, Li XH, Jiang WG, Zhang YC, Xin Y (2003) Growth, invasion, metastasis, differentiation, angiogenesis and apoptosis of gastric cancer regulated by expression of PTEN encoding products. World J Gastroenterol 9:1662–1666